る。偽膜によって眼球結膜と眼瞼結膜が癒着すると眼球運動障害を呈することがある。

III. 原因別による私の処方（第1・第2選択薬，用法・用量）

細菌性結膜炎では，起炎菌に有効な抗生物質の投与を行う。クラミジア結膜炎には，ニューキノロン系抗菌薬（オゼックス®など）の頻回点眼，あるいはタリビッド®眼軟膏1日5回点入を行う。もっとも頻度の高いインフルエンザ菌，肺炎球菌をターゲットにする場合には，広範囲の抗菌スペクトルを有するニューキノロン系抗菌薬（オゼックス®，クラビット®）1回1滴，1日3回点眼を行う。

アデノウイルス性結膜炎に対しては，特別な抗ウイルス薬はなく，混合感染予防のために抗菌点眼薬を用いる。症状が劇症で角膜炎を伴うときにはステロイド点眼薬（リンデロン®点眼液）を用いる。もっとも重要なことは伝染予防対策であり，流水での手洗い，ペーパータオルの使用，学校への出席停止の厳守などである。

アレルギー性結膜炎では，非ステロイド系の抗アレルギー剤（パタノール®1日4回）を投与する。重篤なアレルギー性結膜炎では副腎皮質ステロイド（0.1%フルメトロン®点眼液1日4回）や免疫抑制剤（パピロックミニ®点眼液1日4回）の投与を行う。非眼科医による安易な副腎皮質ステロイドの投与は避けるべきである。

IV. 処方のポイント（治療）

抗菌薬投与による耐性菌の出現に注意が必要である。

V. 副作用とその対策

抗菌薬の重篤な副作用は少なく，眼刺激感，眼周囲についたときのかぶれなどである。

VI. 注意が必要な点

もっとも注意が必要な点としては，結膜炎以外にも充血を主訴とする眼疾患が多数存在することである。角膜炎，虹彩炎，緑内障などでは毛様充血を来す。眼脂を伴わない点，眼瞼結膜に充血がみられない点で結膜炎と異なり，これらを見た場合には眼科医に紹介すべきである。安易に副腎皮質ステロイドの処方を行うと，一時的に症状の改善がみられることが多く，確定診断に難渋することがある。

VII. 治らない患児への対応

ウイルス性結膜炎でなければ，治療によって3日以内に症状の改善があるはずである。眼脂が多い他の疾患として，涙嚢炎や麦粒腫などがあるため，3日以内に改善が見られない場合には眼科医に紹介すべきである。

☆　☆　☆　☆　☆　☆

Negative regulation of ciliary length by ciliary male germ cell-associated kinase (Mak) is required for retinal photoreceptor survival

Yoshihiro Omori[a,b], Taro Chaya[a,b], Kimiko Katoh[a], Naoko Kajimura[c], Shigeru Sato[a,d], Koichiro Muraoka[a], Shinji Ueno[e], Toshiyuki Koyasu[e], Mineo Kondo[e], and Takahisa Furukawa[a,b,1]

[a]Department of Developmental Biology and [b]Japan Science and Technology Agency, Core Research for Evolutional Science and Technology, Osaka Bioscience Institute, 6-2-4 Furuedai, Suita, Osaka 565-0874, Japan; [c]Research Center for Ultra-High Voltage Electron Microscopy, Osaka University, 7-1 Mihogaoka, Ibaraki, Osaka 567-0047, Japan; [d]Department of Ophthalmology, Osaka University Graduate School of Medicine, 2-2 Yamadaoka, Suita, Osaka 565-0871, Japan; and [e]Department of Ophthalmology, Nagoya University Graduate School of Medicine, 65 Tsuruma-cho, Showa-ku, Nagoya 466-8550, Japan

Edited by Jeremy Nathans, The Johns Hopkins University, Baltimore, MD, and approved November 12, 2010 (received for review June 30, 2010)

Cilia function as cell sensors in many organs, and their disorders are referred to as "ciliopathies." Although ciliary components and transport machinery have been well studied, regulatory mechanisms of ciliary formation and maintenance are poorly understood. Here we show that male germ cell-associated kinase (Mak) regulates retinal photoreceptor ciliary length and subcompartmentalization. Mak was localized both in the connecting cilia and outer-segment axonemes of photoreceptor cells. In the *Mak*-null retina, photoreceptors exhibit elongated cilia and progressive degeneration. We observed accumulation of intraflagellar transport 88 (IFT88) and IFT57, expansion of kinesin family member 3A (Kif3a), and acetylated α-tubulin signals in the *Mak*-null photoreceptor cilia. We found abnormal rhodopsin accumulation in the *Mak*-null photoreceptor cell bodies at postnatal day 14. In addition, overexpression of retinitis pigmentosa 1 (RP1), a microtubule-associated protein localized in outer-segment axonemes, induced ciliary elongation, and Mak coexpression rescued excessive ciliary elongation by RP1. The RP1 N-terminal portion induces ciliary elongation and increased intensity of acetylated α-tubulin labeling in the cells and is phosphorylated by Mak. These results suggest that Mak is essential for the regulation of ciliary length and is required for the long-term survival of photoreceptors.

Cilia are evolutionally conserved microtubule-based organelles that extend from basal bodies and form on the apical surface of cells. In humans, ciliary dysfunction is associated with various diseases that can be broadly classified as "ciliopathies." As exemplified by Bardet-Biedl syndrome (BBS), diseases linked with a defect in the primary cilia usually are associated with a broad spectrum of pathologies, including polydactyly, craniofacial abnormalities, brain malformation, situs inversus, obesity, diabetes, polycystic kidney, and retinal degeneration (1, 2). In vertebrates, many types of cells in the G1 phase develop cilia, but ciliary length varies in each cell type of different tissues (3). Retinal photoreceptor cells develop a light-sensory structure containing photopigments and light-transducing machinery, the outer segment. Outer segments are formed initially from the primary cilia in photoreceptor precursors (4, 5). The photoreceptor cilium is divided structurally into at least two subcompartments: the connecting cilia, distal to the basal body, and the axoneme in the outer segment, distal to the connecting cilia. The connecting cilium is analogous to the transitional zone of the motile cilia (6, 7). Connecting cilium connects the inner and outer segments of photoreceptors and is essential for protein transport between the inner and outer segments. Defects of the photoreceptor ciliary transport machinery (called "intraflagellar transport," IFT) cause photoreceptor degeneration in model animals (8–10). The retinitis pigmentosa 1 (RP1) protein is localized specifically in the outer-segment axonemes in photoreceptors, which stabilizes cytosolic microtubules (11). A mutation in human *RP1* generating a deletion of the RP1 C-terminal portion causes dominant retinitis pigmentosa (12).

Mechanisms of ciliogenesis have been well studied in the green algae *Chlamydomonas reinhardtii*. The *Chlamydomonas LF4* mutant shows a long-flagella phenotype. *LF4* encodes a protein highly similar to mammalian male germ cell-associated kinase (Mak) and intestinal cell kinase (ICK) (13). Loss of function of the *LF4* homologs *Caenorhabditis elegans dye-filling defective 5* (*Dyf-5*) and *Leishmania Mexicana LmxMPK9* also causes slightly elongated cilia or flagella (14, 15). However, molecular regulatory mechanisms controlling ciliary length remain unknown. *Mak* was first identified as a gene highly expressed in testicular germ cells (16). Spermatogenesis of the *Mak*-KO mouse is intact (17). In addition to expression in the testis, *Mak* is also expressed in the retina (18, 19). However, the molecular function of Mak in the retina has not been reported yet.

Results

***Mak* Is Expressed in Photoreceptors in the Retina.** In the course of a microarray screening for genes specifically expressed in photoreceptors (20), we found that the *Mak* transcript is markedly reduced in the orthodenticle homeobox 2 (Otx2) conditional knockout (CKO) retina in which most of the photoreceptors are converted to amacrine-like cells (21). We confirmed by quantitative PCR analysis that *Mak* expression is markedly decreased in the *Otx2* CKO retina at postnatal day 12 (P12) (Fig. S1*A*). From a retinal cDNA library we cloned an alternatively spliced form of *Mak* full-length cDNA containing a 75-bp in-frame insertion to the reported *Mak* cDNA (19) (Fig. S2). RT-PCR analysis revealed that this form is likely to be the major alternatively spliced form of the *Mak* transcript in the retina (four of six clones analyzed). To investigate *Mak* expression in the developing retina, we performed in situ hybridization analysis using a *Mak* probe (Fig. 1*A* and *B* and Fig. S1 *B–D*). *Mak* expression was detected first at embryonic day 15.5 (E15.5) in the outer part of the neuroblastic layer (NBL), corresponding to photoreceptor precursors (Fig. 1*A*). *Mak* expression was restricted to the photoreceptor layer after birth (Fig. 1*B* and Fig. S1 *C* and *D*). These results indicate that *Mak* is expressed predominantly in photoreceptor cells in the retina.

Mak Is Localized in the Photoreceptor Connecting Cilia and Outer-Segment Axonemes. To investigate the subcellular localization of Mak in photoreceptor cells, we immunostained retinal sections using an anti-Mak antibody. To eliminate cross-reaction with other kinases, we raised an antibody which recognizes the C-terminal portion of Mak. We confirmed that the anti-Mak antibody

Author contributions: Y.O. and T.F. designed research; Y.O., T.C., K.K., N.K., S.S., K.M., S.U., T.K., M.K., and T.F. performed research; Y.O. and T.F. contributed new reagents/analytic tools; Y.O., T.C., K.K., N.K., S.S., K.M., S.U., T.K., and M.K. analyzed data; and Y.O. and T.F. wrote the paper.

The authors declare no conflict of interest.

This article is a PNAS Direct Submission.

Freely available online through the PNAS open access option.

[1]To whom correspondence should be addressed. E-mail: furukawa@obi.or.jp.

This article contains supporting information online at www.pnas.org/lookup/suppl/doi:10.1073/pnas.1009437108/-/DCSupplemental.

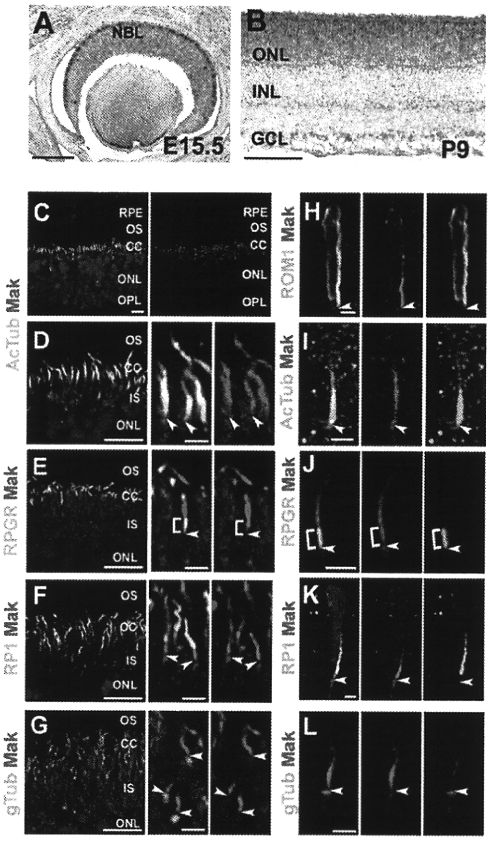

Fig. 1. Expression and subcellular localization of Mak in the retina. (*A* and *B*) In situ hybridization analysis of retinal sections at E15.5 (*A*) and postnatal day 9 (P9) (*B*). *Mak* mRNA is expressed in both photoreceptor precursors and developing photoreceptors in the retina. (*C–L*) Subcellular localization of Mak in photoreceptors. Retinal sections at P14 (*E*) and 1 mo (*C*, *D*, *F*, and *G*) and dissociated photoreceptor cells at P14 (*H–L*) were stained with anti-Mak (red in *C–L*) and anti-acetylated α-tubulin (a marker for cilia; green in *C*, *D*, and *I*), anti-RPGR (a marker for connecting cilia; green in *E* and *J*), anti-RP1 (a marker for outer-segment axonemes; green in *F* and *K*), anti-ROM1 (a marker for outer-segment disks, green in *H*), or anti–γ-tubulin (a marker for basal bodies; green in *G* and *L*) antibodies. [Scale bars: 100 μm (*A* and *B*), 2 μm (*H–L* and *D–G Center* and *Right*), and 10 μm (*C* and *D–G Left*).] Arrowheads (*D–L*) indicate basal body-connecting cilium junctions. Brackets (*E* and *J*) indicate connecting cilia. CC, connecting cilia; GCL, ganglion cell layer; INL, inner nuclear layer; IS, inner segments; NBL, neuroblastic layer; ONL, outer nuclear layer; OPL, outer plexiform layer OS, outer segments; RPE, retinal pigment epithelium.

recognizes the major retinal variant of Mak with the 25-amino acid insertion (Fig. S1*E*). By immunostaining, we observed a layer of Mak signals between the retinal pigment epithelia and outer nuclear layer (ONL) corresponding to the photoreceptor cilia (Fig. 1*C*).

To identify the precise localization of Mak in the photoreceptor cilia, we immunostained the retina using the Mak antibody along with other ciliary markers including acetylated α-tubulin (a ciliary marker), retinitis pigmentosa GTPase regulator (RPGR, a connecting cilium marker) (7), RP1 (a marker for the outer-segment axonemes) (11), and rod outer-segment membrane protein 1 (ROM1, a marker for the outer-segment disks) (Fig. 1 *C–L*) (22). The Mak signal was observed broadly in the photoreceptor cilia overlapping with ROM1, RPGR, RP1 and acetylated α-tubulin signals (Fig. 1 *C–F* and *H–K*; for summary, see Fig. S9). We observed a slight signal of Mak overlapping with the γ-tubulin signal, a marker for basal bodies (Fig. 1 *G* and *L*). These results indicate that Mak is localized in both the connecting cilia and the outer-segment axonemes. Interestingly, the intensity of the Mak signal was not uniform in the photoreceptor cilia. The decreased Mak signal was observed in the proximal portion of the connecting cilia (Fig. 1 *E* and *J*) and the distal portion of the outer-segment axonemes (Fig. 1 *F* and *K*).

Photoreceptors Degenerate Progressively in the *Mak*-Deficient Retina. *Mak*-null mice were established previously, and it was reported that *Mak* is not essential for spermatogenesis, although *Mak* is highly expressed in the testis (17). To investigate in vivo Mak function in the retina, we analyzed this KO mouse. We confirmed that none of the normal *Mak* transcripts, including the major retinal variant of *Mak* with a 75-bp insertion, were expressed in the *Mak*-KO retina (Fig. S1*F*). Until retinogenesis was complete in the normal retina at postnatal day 14 (P14), the *Mak*-KO retina exhibited normal layering and cell composition, indicating that loss of *Mak* does not affect cell fates (Fig. 2 *A* and *B* and Fig. S3 *A–F*). We also analyzed the retinas at age 1 mo, 6 mo, and 12 mo. Notably, we found progressive degeneration of the ONL (a photoreceptor layer) in the *Mak*-KO retina after 1 mo (Fig. 2 *C–I*). This progressive ONL loss often is observed in animal models of retinitis pigmentosa and Leber's congenital amaurosis (23–27). We observed no obvious structural differences between the heterozygous and wild-type retinas at 6 mo (Fig. S4 *A–C*). The thickness of the other layers did not differ in the *Mak*-KO and wild-type retinas (Fig. S5*A*).

To examine if loss of *Mak* in the retina affects photoreceptor function, we recorded electroretinograms (ERG) from adult *Mak*-KO mice at age 3 mo. Both scotopic and photopic ERG amplitudes of *Mak*-KO mice were significantly smaller than those of the control mice (Fig. 2*J* and Fig. S5 *B–D*). These results show that the loss of *Mak* impairs the function of both rods and cones.

Cilia Are Elongated in *Mak*-KO Photoreceptors. How does progressive photoreceptor death occur in the *Mak*-KO retina? To explore this question, we examined photoreceptors in the *Mak*-deficient retina by immunostaining using antibodies against photoreceptor ciliary markers. We first confirmed the loss of *Mak* in the photoreceptor cilia of the *Mak*-KO retina at P14 (Fig. 3 *A*, *A′*, *B*, and *B′*). Notably, we found that the cilia stained with the anti-acetylated α-tubulin antibody were markedly elongated in *Mak*-deficient rod photoreceptors (Fig. 3*B*). We measured ciliary length of rod photoreceptors and found that the acetylated α-tubulin–positive cilia in *Mak*-KO photoreceptors were approximately twice the length of wild-type cilia (Fig. 3 *K* and *L*). We also found that cone photoreceptor cilia were elongated in the *Mak*-null retina (Fig. S6 *A–D*). To investigate whether ciliary subcompartments are affected in *Mak*-KO photoreceptors, we immunostained for RPGR (a marker of the connecting cilia) in the *Mak*-KO retina. We observed an approximately twofold elongation of the RPGR-positive connecting cilia in the *Mak*-KO retina (Fig. 3 *C*, *D*, and *L* and Fig. S6*E*). In contrast, γ-tubulin staining (a basal body marker) showed no significant difference between *Mak*-KO and wild-type photoreceptors (Fig. 3 *C* and *D*). Next, we stained for RP1, a marker of the outer-segment axonemes. Unexpectedly, we observed excessively long acetylated α-tubulin labeling in the outer-segment axonemes (Fig. 3 *E* and *F*). In most of the wild-type photoreceptors, an acetylated α-tubulin signal is observed in less than half of the proximal portion of the RP1-positive outer-segment axoneme, whereas in the *Mak*-KO photoreceptors often almost all the outer-segment axoneme is acetylated α-tubulin signal-positive. The percentage of excessively long acetylated α-tubulin labeling of the outer-segment axonemes (wherein more than half of the distal portion of the outer-segment axoneme is acetylated α-tubulin signal-positive) is 5.1% (n = 59) in the wild-type photoreceptors, whereas in *Mak*-KO photoreceptors 83.3% (n = 66) of the axonemes have excessively long acetylated α-tubulin labeling. The distance from the top of the outer segment to the top of the outer-segment axonemes stained with acetylated α-tubulin decreased in *Mak*-KO photoreceptors (Fig. S6 *F* and *G*). These results demonstrate that loss of *Mak* affects both subcompartments of the cilia, the connecting cilia and outer-segment axonemes.

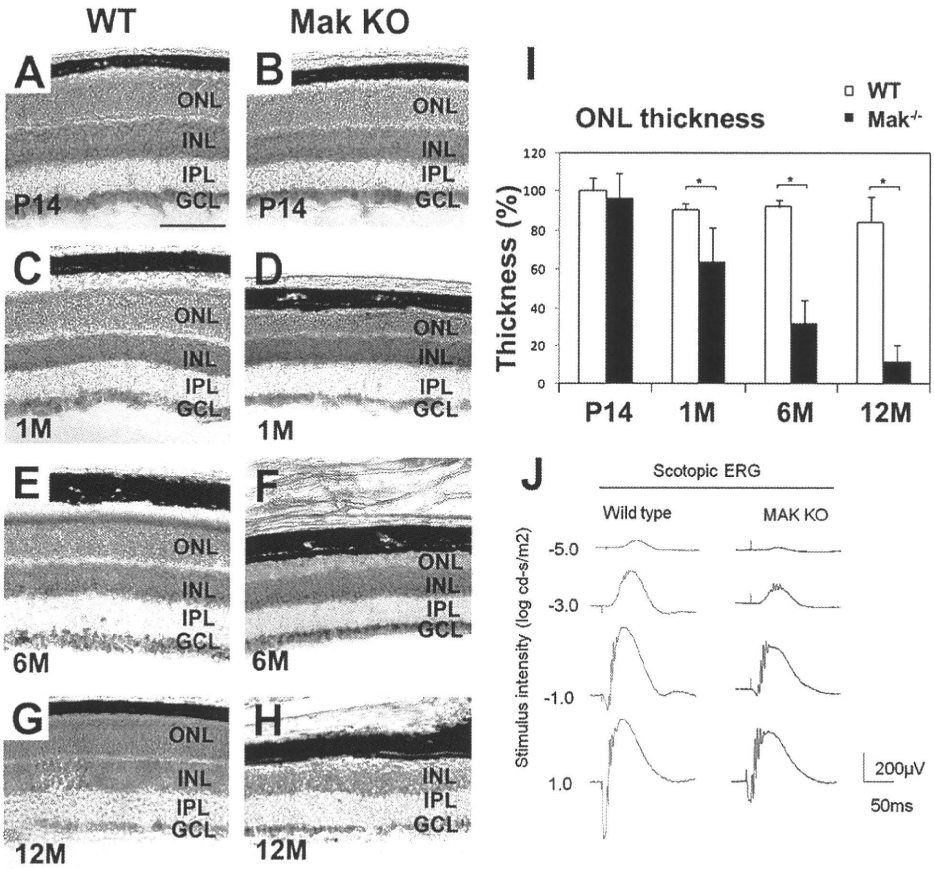

Fig. 2. Loss of *Mak* leads to photoreceptor degeneration (*A–H*). Retinal sections from wild-type and *Mak*-KO mice at age P14 (*A* and *B*), 1 mo (*C* and *D*), 6 mo (*E* and *F*), and 12 mo (*G* and *H*) were stained with toluidine blue. Progressive degeneration of the ONL (a photoreceptor layer) occurs in the *Mak*-KO retina. (Scale bar: 100 μm.) IPL, inner plexiform layer. (*I*) Thickness of retinal layers was measured at age P14, 1 mo, 6 mo, and 12 mo. ONL thickness decreased progressively in the *Mak*-KO retina. Average of layer thickness in the wild-type retina at P14 was set to 100%. Error bars show SD. $*P < 0.03$. (*J*) ERGs recorded from *Mak*-KO mice. Scotopic ERGs elicited by four different stimulus intensities (−5.0 to 1.0 log cd-s/m^2).

To examine whether loss of *Mak* affects the anterograde IFT and kinesin motors, we stained photoreceptor cilia with anti-IFT88, anti-IFT57, and anti-Kif3a antibodies. We observed that both IFT88 and IFT57 were concentrated on two portions, the tip of the connecting cilia at the outer-segment base and the basal part of the connecting cilia, as previously reported (28). Notably, in *Mak*-KO photoreceptors, we found that IFT88 and IFT57 were accumulated in outer-segment axonemes (Fig. 3 *G* and *H* and Fig. S6 *H* and *I*). In wild-type photoreceptors, the Kif3a staining overlaps with the acetylated α-tubulin staining and is concentrated on the basal part of the cilia (Fig. S6 *J* and *K*). In *Mak*-KO photoreceptors, the Kif3a staining extends along the elongated acetylated α-tubulin–positive cilia (Fig. S6 *J* and *K*). Interestingly, we also observed an accumulation of rhodopsin in the *Mak*-KO photoreceptor cell bodies at P14 (Fig. 3 *I*, *I′*, *J*, and *J′*).

Mak is expressed in epithelia of the nasal cavity and the testis (16, 19). Respiratory epithelia of the nasal cavity have multiple motile cilia which display the 9+2 microtubule structure. We observed Mak localizing in the cilia of the respiratory epithelia (Fig. S6*L*). The Mak signal is reduced in the *Mak*-KO nasal cavity (Fig. S6*M*). However, the ciliary length of respiratory epithelia did not differ in wild-type and *Mak*-KO mice (Fig. S6 *L–N*). Similarly, we also found that the acetylated-α-tubulin–positive flagellar length of epididymal sperm does not differ in wild-type and *Mak*-KO mice (Fig. S6 *O–Q*).

Aberrant Outer-Segment Disk Formation in *Mak*-Deficient Photoreceptors. The 9+0 axonemes of the photoreceptor cilia are assembled by nine peripheral doublet microtubules without a central microtubule (3). To test if loss of *Mak* affects ultrastructural microtubule organization in the photoreceptor cilia, we performed an electron microscopic analysis. We observed no significant change in ciliary ultrastructures, including the array of the 9+0 microtubule doublets in transverse sections of the connecting cilium in *Mak*-KO photoreceptors (Fig. S7 *A* and *B*). Consistent with the results of the immunofluorescent analysis, we found elongated connecting cilium in the *Mak*-KO photoreceptors at age 1 mo in a longitudinal section of the connecting cilia ($100 \pm 2\%$ in wild type, $n = 12$; $233 \pm 22\%$ in *Mak*-KO, $n = 9$; $P < 0.03$) (Fig. 3 *M* and *N*).

In both vertebrate photoreceptors and nematode amphid channel cilia, the proximal microtubules of the axonemes are doublets, whereas distal microtubules are singlets (29, 30). In the distal segment of the amphid channel cilia in *dyf-5* animals, singlet microtubules were observed (14). We observed singlet microtubules in outer-segment axonemes, which are positioned near the disk clefts, in both wild-type and Mak-null retinas (Fig. S7 *C–F*).

We observed severely disorganized *Mak*-KO outer segments at age 1 mo compared with the wild type (Fig. 3 *M* and *N*). In contrast, disk rim formation seems to be intact in the *Mak*-null outer segments at age 1 mo (Fig. S7 *G* and *H*). To examine whether the outer-segment disorganization observed in Mak-deficient retinas is caused by a developmental defect or degeneration after normal development, we observed photoreceptor outer segments at P14 by electron microscopy. At this stage, the outer segments are still developing (31). In wild-type photoreceptors, the stack of disk membranes in the outer segments is oriented perpendicular to the long axis of the outer segments (Fig. S7 *I* and *I′*). In the *Mak*-KO retina, however, we observed that the disk membranes were frequently oriented obliquely or parallel to the long axis of the outer segments (Fig. S7 *J* and *J′*). In addition, the disk diameters are approximately two to four times larger in *Mak*-null than in wild-type outer segments (Fig. S7 *I′* and *J′*). Enlarged disks oriented obliquely or parallel to the long axis of photoreceptors were reported in mutant mice including *RP1*-mutant and *RPGRIP1*-null mice (24, 25). These results suggest the disorganization of the outer segment observed in the *Mak*-KO retinas is, at least partially, the result of a developmental defect in outer-segment formation.

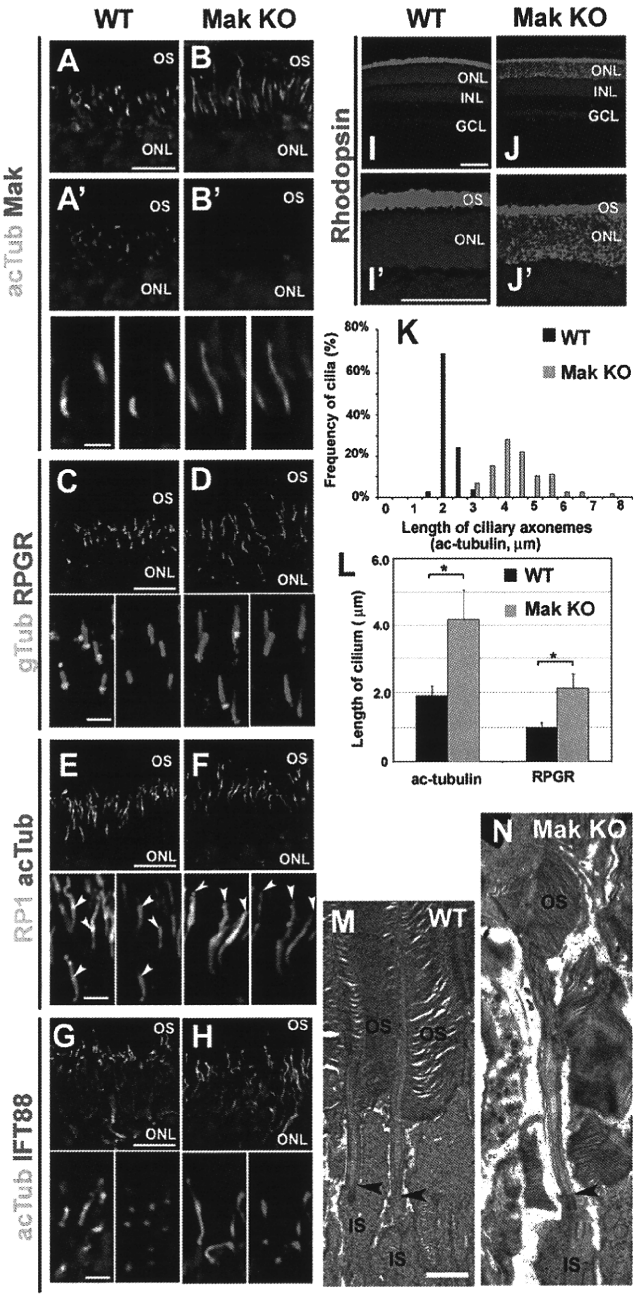

Fig. 3. Ciliary defect in *Mak*-null photoreceptors. (*A–H*) Immunohistochemical analysis of the *Mak*-null photoreceptor cilia. Retinal sections from wild-type mice (*A*, *A'*, *C*, *E*, and *G*) and *Mak*-KO mice (*B*, *B'*, *D*, *F*, and *H*) at age P14 (*A*, *A'*, *B*, and *B'*) and 1 mo (*C–H*) were stained with anti-Mak (red in *A*, *A'*, *B*, and *B'*), anti-acetylated α-tubulin (a ciliary marker; green in *A*, *B*, *G*, and *H*; red in *E* and *F*), anti-RPGR (a connecting cilium marker; red in *C* and *D*), anti-RP1 (a marker for the outer-segment axonemes; green in *E* and *F*), anti-IFT88 (a component of IFT complex; red in *G* and *H*) or anti–γ-tubulin (a marker for the basal bodies; green in *C* and *D*) antibodies. Arrowheads in *E* and *F* indicate the distal tips of acetylated microtubules in the outer-segment axonemes. (*I* and *J*) Rhodopsin is mislocalized in the *Mak*-KO retina. Retinal sections from wild-type mice (*I* and *I'*) and *Mak*-KO mice (*J* and *J'*) at age P14 were stained with an anti-rhodopsin antibody. [Scale bars: 10 μm (*A*, *C*, *E*, and *G*, *Upper*), 100 μm (*I* and *I'*), and 2 μm (*A'*, *C*, *E*, and *G*, *Lower*).] (*K* and *L*) Length of the ciliary axonemes stained with the anti-acetylated α-tubulin antibody (*K* and *L*) and connecting cilia stained with the anti-RPGR (*L*) antibody in the wild-type photoreceptors (black bars) and *Mak*-KO photoreceptors (gray bars) were measured. Error bars show SE. $*P < 0.03$. (*M* and *N*) Longitudinal profiles of the connecting cilia in 1-mo-old wild-type photoreceptors (*M*) and *Mak*-KO photoreceptors (*N*) observed by electron microscopy. Arrowheads indicate the basal body-connecting cilium junctions in the photoreceptors. (Scale bar in *M*: 1 μm.)

Mak Overexpression Reduces Ciliary Elongation in Cultured Cells. To investigate the mechanisms by which Mak regulates ciliary length, we established a cultured cell system in which NIH 3T3 fibroblast cells develop cilia at a high frequency within 24 h after serum starvation (Fig. S8). We prepared FLAG-tagged constructs expressing a full-length wild-type Mak (*Mak-WT*), a kinase-dead mutant Mak (*Mak-KD*), and a deletion-mutant Mak lacking the C-terminal nonkinase domain (*Mak-N*) (Fig. S8*F*). The *Mak-KD* construct was generated by replacing a lysine residue (K33) located in the ATP-binding pocket of the Mak kinase domain with an arginine residue (32).

We transfected these constructs into NIH 3T3 cells and measured ciliary length. We found that the cells transfected with the wild-type *Mak* construct had shorter cilia than cells transfected with the control constructs (Fig. S8 *A*, *B*, and *G*). On the other hand, cells transfected with the *Mak-KD* or *Mak-N* construct showed no significant change in ciliary length (Fig. S8 *D*, *E*, and *G*), showing that kinase activity and/or the C-terminal region of Mak is essential for the regulation of ciliary length.

We then investigated the subcellular localization of Mak in transfected cells using an anti-FLAG antibody. We observed that *Mak-WT* was localized mainly in the nuclei as previously reported (32). As expected from the ciliary localization of Mak in photoreceptors, we observed that *Mak-WT* is also localized in the cilia of transfected cells. Mak localization was restricted to the tip of the shortened cilia (Fig. S8*B*). Although we rarely observed elongated cilia in *Mak-WT*–transfected cells, ciliary tip localization of *Mak-WT* was observed in those cells (Fig. S8*C*). We found that *Mak-KD* is also localized at the ciliary tip, suggesting that kinase activity is not required for the ciliary localization of Mak. In contrast, *Mak-N* was not localized in the cilia, showing that the C-terminal portion of Mak is essential for the ciliary localization of Mak.

RP1 Induces Ciliary Elongation and Reduces the Effect of Mak Overexpression. It was previously reported that knock-in mice with a partial deletion of the *RP1* gene exhibited shorten cilia (24). As we described above, we found colocalization of Mak with RP1 in the ciliary axoneme of wild-type photoreceptors. *Mak*-KO photoreceptors exhibited excessively long acetylated α-tubulin labeling. These observations prompted us to investigate whether RP1 is involved in the mechanisms by which Mak regulates ciliary length. To do so, we prepared constructs expressing RP1 and transfected them with or without the Mak-expressing constructs (Fig. 4*A*). We observed increased ciliary length in the cells transfected with full-length RP1 (*RP1-FL*) (Fig. 4 *B–E*, *J*, and *K*). In humans, the mutations in the *RP1* gene generating deletion of the C-terminal portion of RP1 cause dominant retinitis pigmentosa (12). Interestingly, the intensity of acetylated α-tubulin labeling significantly increased in cells expressing the N-terminal RP1 (RP1-N) construct containing the doublecortin domain, indicating that the cytoplasmic microtubules are more stable in these cells (Fig. 4 *F–I*). Coimmunostaining of FLAG-tag with acetylated α-tubulin showed that RP1-FL and RP1-N were localized in a large portion of the distal cilia but not in the basal cilia, a putative transition zone (Fig. 4 *E* and *G*). These results suggest that RP1 is a positive regulator of ciliary length. Notably, cotransfection of *Mak* with *RP1-FL* or *RP1-N* constructs rescued the excessive elongation of the cilia (Fig. 4 *J* and *K*). This result suggests that a functional balance between Mak and RP1 is essential for the regulation of ciliary length and proper formation of the ciliary subcompartments. To test whether Mak rescues increased acetylated α-tubulin signals in cells expressing RP1-N, we cotransfected Mak with an RP1-N construct and observed the acetylated α-tubulin signal levels in the cells. We found that expression of Mak significantly decreased the intensity of acetylated α-tubulin labeling in the cells expressing RP1-N (Fig. S8 *H–J*).

To assess whether Mak physically interacts with RP1, we performed an immunoprecipitation assay. We expressed Mak and FLAG-tagged full-length RP1 or RP1-N in HEK293 cells and performed an immunoprecipitation with an anti-FLAG antibody. We found specific interactions of Mak with both RP1-FL and RP1-N (Fig. 4*L*).

Then, to examine the possibility that Mak directly phosphorylates RP1, we performed a kinase assay using purified GST-Mak. Interestingly, we found that GST-RP1-N was markedly phosphorylated by Mak, whereas no obvious phosphorylation of the GST-RP1 C-terminal (GST-RP1-C1) construct or GST alone was detected (Fig. 4*M*). We observed weak phosphorylation of GST-RP1-C2 by Mak. To characterize the kinase activity of Mak with the RP1-N substrate, we performed a kinetic analysis. We found that the K_m value for ATP was 19 μM (Fig. S8*K*). In addition, we confirmed that Mak-phosphorylated RP1-N was dephosphorylated by λ-phosphatase (Fig. S8*L*). These results support the idea that RP1 is a phosphorylation target of Mak.

Discussion

In the current study, we show that Mak is essential for preventing excessive elongation of the cilia and for maintenance of photoreceptor cells. Our observations in the *Mak*-KO retina suggest that a negative regulatory mechanism of ciliary length is essential for long-term photoreceptor survival, suggesting that this mechanism is involved in the pathogenesis of human photoreceptor degenerative diseases such as retinitis pigmentosa, Leber's congenital amaurosis, and BBS. In addition, similar negative regulatory mechanisms of ciliary length might be involved in the pathogenesis of other ciliopathies including polydactyly, craniofacial abnormalities, brain malformation, situs inversus, obesity, diabetes, and polycystic kidney (1, 2).

How does the aberrant ciliary elongation in *Mak*-KO photoreceptors induce progressive photoreceptor death? One possible explanation is that the abnormally elongated cilia affect protein transport from the inner segments to the outer segments in photoreceptors, resulting in photoreceptor degeneration. Several lines of evidence support this idea. We observed an accumulation of rhodopsin in the *Mak*-KO photoreceptor cell bodies in the retina at P14. The transport efficiency of rhodopsin from the inner to the outer segments through the connecting cilia would be reduced in *Mak*-KO photoreceptors. Mutations in rhodopsin or protein transport machinery of the cilia (e.g., *Kif3a* or *IFT* mutants) cause accumulation of rhodopsin in the photoreceptor cell body and result in photoreceptor cell death. Absence of *Dyf-5*, a nematode homolog of *Mak*, affects the motility of kinesin motors and IFT particles in the cilia (14). Similarly, we identified aberrant accumulations of IFT and kinesin in the Mak-KO photoreceptor cilia. Mak may regulate ciliary transport by directly phosphorylating the components of ciliary transport machinery including kinesin and dynein motors, IFT particles, and/or BBSomes (1, 3, 33).

We demonstrate that overexpression of wild-type *RP1* induces ciliary elongation. In addition, expression of the N-terminal portion of RP1 induces an increased intensity of acetylated α-tubulin labeling in cultured cells. These results suggest that excess activation of the microtubule-associated protein RP1 can induce excess ciliary elongation. The evidence shown here supports the idea

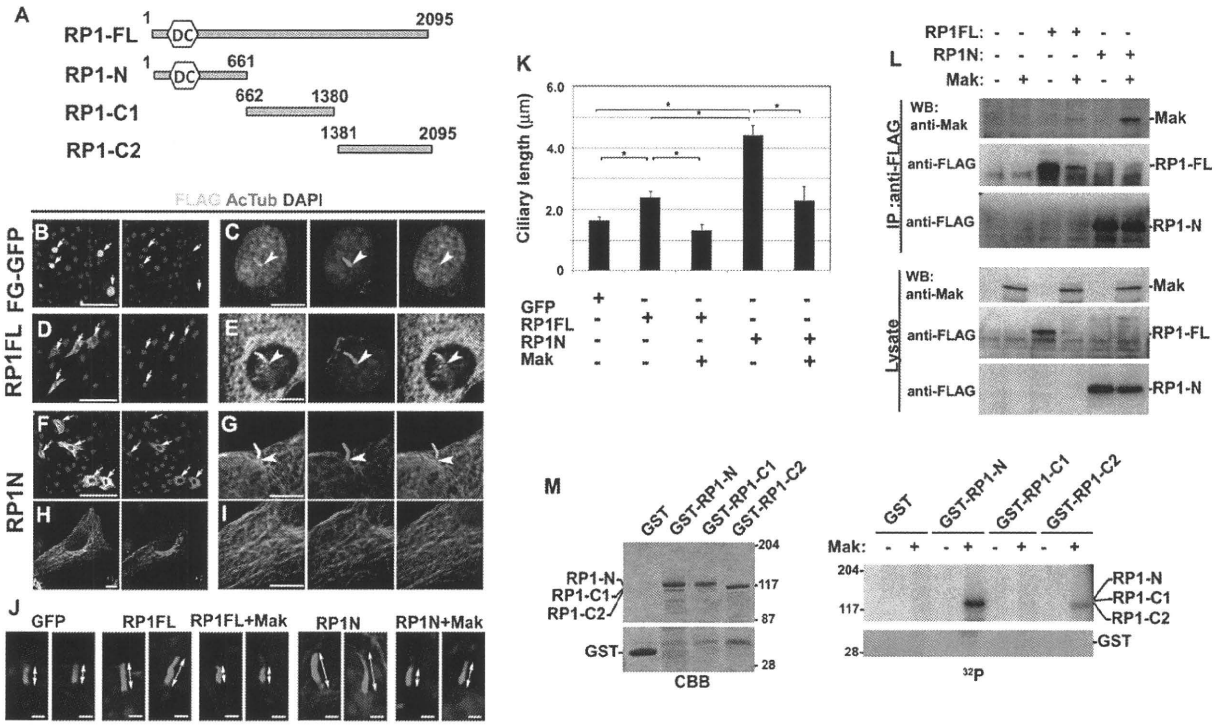

Fig. 4. RP1 controls ciliary length and is phosphorylated by Mak. (*A–I*) Overexpression of RP1 induces ciliary elongation. (*A*) Schematic diagrams of the RP1-FL, -N, -C1 and -C2 constructs. DC, doublecortin domain. (*B–I*) FLAG-tagged constructs expressing GFP (*B* and *C*), RP1-FL (*D* and *E*) or RP1 lacking the C-terminal portion (RP1-N) (*F–I*) were transfected into NIH 3T3 cells. Localization of FLAG-tagged proteins was observed using anti-FLAG (green) and anti-acetylated α-tubulin (red) antibodies and DAPI (blue). Arrows indicate transfected cells. Arrowheads indicate basal part of cilia. (*J* and *K*) RP1 and Mak antagonistically regulate ciliary length. FLAG-tagged constructs expressing GFP, RP1-FL, or RP1-N were transfected with or without a *Mak* expression plasmid into NIH 3T3 cells. (*J*) Cilia were observed using the anti-acetylated α-tubulin (red) antibody. (*K*) The length of the cilia stained with the anti-acetylated α-tubulin antibody ($n > 30$ for each construct). Error bars show SE. $^*P < 0.03$. (*L*) Mak interacts with RP1. A Mak expression plasmid was transfected with or without FLAG-tagged RP1 expression plasmids (RP1-FL or RP1-N) into HEK293 cells. RP1 proteins were immunoprecipitated with the anti-FLAG antibody. Immunoprecipitated Mak was detected by Western blotting analysis using the anti-Mak antibody. (*M*) Mak phosphorylates RP1 in vitro. GST-RP1-N (residues 1–661), GST-RP1-C1 (residues 662–1,380), and GST-RP1-C2 (residues 1,381–2,095) were purified from bacterial extracts and stained with Coomassie brilliant blue (CBB) (*Left*). GST-RP1 deletion proteins were applied for the in vitro kinase assay using purified GST-Mak (*Right*). [Scale bars: 100 μm (*B, D,* and *F*), 10 μm (*C, E, G, H,* and *I*), and 2 μm (*J*).]

that Mak regulates ciliary elongation through RP1 phosphorylation. First, we observed that coexpression of Mak with the RP1 constructs rescued the excess ciliary elongation. Second, we identified that Mak phosphorylates the N-terminal portion of RP1, which contains the doublecortin domain. This domain was originally identified in Doublecortin, whose mutations cause X-linked lissencephaly and double cortex syndrome in humans (34). Interestingly, phosphorylation of Doublecortin by several kinases, including JNK, protein kinase A, and cyclin-dependent kinase 5, was shown to regulate affinity to microtubules and migration of neurons (35, 36). Similarly, it is possible that phosphorylation of RP1 by Mak regulates microtubule stability and controls ciliary length (Fig. S9). Retinitis pigmentosa 1-like 1 (RP1L1), a putative microtubule-associated protein, is another candidate for phosphorylation by Mak (37). In contrast to the restricted localization of RP1 in the axonemes of the outer segments, RP1L1 is localized both in the connecting cilium and the outer-segment axoneme, suggesting its involvement in the mechanisms regulating the length of connecting cilium in photoreceptors. How does Mak affect the intensity of acetylated α-tubulin labeling in the cilia? The first possibility is that the change of microtubule-binding status of microtubule-associated proteins by phosphorylation leads to the activation of enzymes involved in microtubule acetylation or deacetylation, because several microtubule-associated proteins were reported to induce microtubule acetylation (38). The second possibility is that Mak directly regulates enzymes involved in microtubule acetylation and/or deacetylation. It was reported that Aurora A regulates ciliary disassembly before cell-cycle entry through phosphorylation of tubulin deacetylase, histone deacetylase 6 (HDAC6). Phosphorylated by Aurora A, HDAC6 deacetylates microtubules of the cilia and facilitates disassembly of the cilia (39). Furthermore, microtubule acetylation causes the recruitment of the molecular motors dynein and kinesin to microtubules (40). In the developing photoreceptor cilia, regulatory balance of acetylation and deacetylation of ciliary microtubules seems to be important for keeping proper ciliary length and/or ciliary transport machinery. Mak may regulate this balance by phosphorylation of these molecules.

Materials and Methods

Animals. We used *Mak*-KO mice with a deletion of exons 5–8 in the Mak genomic locus which encodes the catalytic kinase domain and the proline and glutamine-rich domain as previously reported (17). The Mak-KO mouse strain was provided by RIKEN BioResource Center through the National BioResource Project of the Japanese Government Ministry of Education, Culture, Sports, Science and Technology. Reagents and procedures are described in detail in *SI Materials and Methods*.

ACKNOWLEDGMENTS. We thank Drs. Y. Shinkai (Kyoto University), T. Li (National Institutes of Health), E. A. Pierce (University of Pennsylvania School of Medicine), J. Zuo (St. Jude Children's Research Hospital, Utah), T. Yamashita (St. Jude Children's Research Hospital), G. J. Pazour (University of Massachusetts Medical School), J. C. Besharse (Medical College of Wisconsin), and H. J. Kung (University of California, Davis) for reagents and technical advice. We thank M. Kadowaki, M. Joukan, A. Tani, T. Tsujii, A. Ishimaru, Y. Saioka, K. Sone, and S. Kennedy for technical assistance. This work was supported by Core Research for Evolutional Science and Technology and Precursory Research for Embryonic Science and Technology from the Japan Science and Technology Agency, a grant from Molecular Brain Science, Grants-in-Aid for Scientific Research on Priority Areas and a Grant-in-Aid for Scientific Research (B), Young Scientists (B), the Takeda Science Foundation, the Uehara Memorial Foundation, Novartis Foundation, Senri Life Science Foundation, Kato Memorial Bioscience Foundation, the Naito Foundation, Mochida Memorial Foundation for Medical and Pharmaceutical Research, and the Japan National Society for the Prevention of Blindness.

1. Gerdes JM, Davis EE, Katsanis N (2009) The vertebrate primary cilium in development, homeostasis, and disease. *Cell* 137:32–45.
2. Nigg EA, Raff JW (2009) Centrioles, centrosomes, and cilia in health and disease. *Cell* 139:663–678.
3. Fliegauf M, Benzing T, Omran H (2007) When cilia go bad: Cilia defects and ciliopathies. *Nat Rev Mol Cell Biol* 8:880–893.
4. Tokuyasu K, Yamada E (1959) The fine structure of the retina studied with the electron microscope. IV. Morphogenesis of outer segments of retinal rods. *J Biophys Biochem Cytol* 6:225–230.
5. Rosenbaum JL, Witman GB (2002) Intraflagellar transport. *Nat Rev Mol Cell Biol* 3: 813–825.
6. Röhlich P (1975) The sensory cilium of retinal rods is analogous to the transitional zone of motile cilia. *Cell Tissue Res* 161:421–430.
7. Hong DH, et al. (2003) RPGR isoforms in photoreceptor connecting cilia and the transitional zone of motile cilia. *Invest Ophthalmol Vis Sci* 44:2413–2421.
8. Marszalek JR, et al. (2000) Genetic evidence for selective transport of opsin and arrestin by kinesin-II in mammalian photoreceptors. *Cell* 102:175–187.
9. Pazour GJ, et al. (2002) The intraflagellar transport protein, IFT88, is essential for vertebrate photoreceptor assembly and maintenance. *J Cell Biol* 157:103–113.
10. Omori Y, et al. (2008) Elipsa is an early determinant of ciliogenesis that links the IFT particle to membrane-associated small GTPase Rab8. *Nat Cell Biol* 10:437–444.
11. Liu Q, Zuo J, Pierce EA (2004) The retinitis pigmentosa 1 protein is a photoreceptor microtubule-associated protein. *J Neurosci* 24:6427–6436.
12. Pierce EA, et al. (1999) Mutations in a gene encoding a new oxygen-regulated photoreceptor protein cause dominant retinitis pigmentosa. *Nat Genet* 22:248–254.
13. Berman SA, Wilson NF, Haas NA, Lefebvre PA (2003) A novel MAP kinase regulates flagellar length in Chlamydomonas. *Curr Biol* 13:1145–1149.
14. Burghoorn J, et al. (2007) Mutation of the MAP kinase DYF-5 affects docking and undocking of kinesin-2 motors and reduces their speed in the cilia of Caenorhabditis elegans. *Proc Natl Acad Sci USA* 104:7157–7162.
15. Bengs F, Scholz A, Kuhn D, Wiese M (2005) LmxMPK9, a mitogen-activated protein kinase homologue affects flagellar length in Leishmania mexicana. *Mol Microbiol* 55:1606–1615.
16. Matsushime H, Jinno A, Takagi N, Shibuya M (1990) A novel mammalian protein kinase gene (mak) is highly expressed in testicular germ cells at and after meiosis. *Mol Cell Biol* 10:2261–2268.
17. Shinkai Y, et al. (2002) A testicular germ cell-associated serine-threonine kinase, MAK, is dispensable for sperm formation. *Mol Cell Biol* 22:3276–3280.
18. Blackshaw S, et al. (2004) Genomic analysis of mouse retinal development. *PLoS Biol* 2: E247.
19. Bladt F, Birchmeier C (1993) Characterization and expression analysis of the murine rck gene: A protein kinase with a potential function in sensory cells. *Differentiation* 53:115–122.
20. Sato S, et al. (2008) Pikachurin, a dystroglycan ligand, is essential for photoreceptor ribbon synapse formation. *Nat Neurosci* 11:923–931.
21. Nishida A, et al. (2003) Otx2 homeobox gene controls retinal photoreceptor cell fate and pineal gland development. *Nat Neurosci* 6:1255–1263.
22. Bascom RA, et al. (1992) Cloning of the cDNA for a novel photoreceptor membrane protein (rom-1) identifies a disk rim protein family implicated in human retinopathies. *Neuron* 8:1171–1184.
23. Hong DH, et al. (2000) A retinitis pigmentosa GTPase regulator (RPGR)-deficient mouse model for X-linked retinitis pigmentosa (RP3). *Proc Natl Acad Sci USA* 97:3649–3654.
24. Liu Q, Lyubarsky A, Skalet JH, Pugh EN, Jr, Pierce EA (2003) RP1 is required for the correct stacking of outer segment discs. *Invest Ophthalmol Vis Sci* 44:4171–4183.
25. Zhao Y, et al. (2003) The retinitis pigmentosa GTPase regulator (RPGR)- interacting protein: Subserving RPGR function and participating in disk morphogenesis. *Proc Natl Acad Sci USA* 100:3965–3970.
26. Mykytyn K, et al. (2004) Bardet-Biedl syndrome type 4 (BBS4)-null mice implicate Bbs4 in flagella formation but not global cilia assembly. *Proc Natl Acad Sci USA* 101:8664–8669.
27. Ross AJ, et al. (2005) Disruption of Bardet-Biedl syndrome ciliary proteins perturbs planar cell polarity in vertebrates. *Nat Genet* 37:1135–1140.
28. Sedmak T, Wolfrum U (2010) Intraflagellar transport molecules in ciliary and nonciliary cells of the retina. *J Cell Biol* 189:171–186.
29. Insinna C, Besharse JC (2008) Intraflagellar transport and the sensory outer segment of vertebrate photoreceptors. *Dev Dyn* 237:1982–1992.
30. Insinna C, Pathak N, Perkins B, Drummond I, Besharse JC (2008) The homodimeric kinesin, Kif17, is essential for vertebrate photoreceptor sensory outer segment development. *Dev Biol* 316:160–170.
31. LaVail MM (1973) Kinetics of rod outer segment renewal in the developing mouse retina. *J Cell Biol* 58:650–661.
32. Xia L, et al. (2002) Identification of human male germ cell-associated kinase, a kinase transcriptionally activated by androgen in prostate cancer cells. *J Biol Chem* 277:35422–35433.
33. Nachury MV, et al. (2007) A core complex of BBS proteins cooperates with the GTPase Rab8 to promote ciliary membrane biogenesis. *Cell* 129:1201–1213.
34. des Portes V, et al. (1998) A novel CNS gene required for neuronal migration and involved in X-linked subcortical laminar heterotopia and lissencephaly syndrome. *Cell* 92:51–61.
35. Schaar BT, Kinoshita K, McConnell SK (2004) Doublecortin microtubule affinity is regulated by a balance of kinase and phosphatase activity at the leading edge of migrating neurons. *Neuron* 41:203–213.
36. Tanaka T, et al. (2004) Cdk5 phosphorylation of doublecortin ser297 regulates its effect on neuronal migration. *Neuron* 41:215–227.
37. Yamashita T, et al. (2009) Essential and synergistic roles of RP1 and RP1L1 in rod photoreceptor axoneme and retinitis pigmentosa. *J Neurosci* 29:9748–9760.
38. Takemura R, et al. (1992) Increased microtubule stability and alpha tubulin acetylation in cells transfected with microtubule-associated proteins MAP1B, MAP2 or tau. *J Cell Sci* 103:953–964.
39. Pugacheva EN, Jablonski SA, Hartman TR, Henske EP, Golemis EA (2007) HEF1-dependent Aurora A activation induces disassembly of the primary cilium. *Cell* 129:1351–1363.
40. Dompierre JP, et al. (2007) Histone deacetylase 6 inhibition compensates for the transport deficit in Huntington's disease by increasing tubulin acetylation. *J Neurosci* 27:3571–3583.

Jpn J Ophthalmol 2010;54:622–637

LETTERS

A Case of Fukuyama Congenital Muscular Dystrophy Associated with Negative Electroretinograms

Fukuyama congenital muscular dystrophy (FCMD) is a congenital dystrophy associated with brain and eye abnormalities.[1] FCMD is an autosomal recessive disorder and occurs only in Japanese. Common ocular findings are optic atrophy, high myopia, cataracts, and weakness of the orbicularis muscles.[1] Abnormal vascular anastomosis and avascularization in the peripheral retina have also been reported. The eyes are only occasionally affected severely, for example, with retinal detachment and microphthalmia.

It was originally believed that patients with FCMD had normal electroretinograms (ERGs),[2] although a slight reduction of the b-wave and reduced ERGs under photopic conditions have been reported.[3,4] We describe an infant with FCMD exhibiting a severe form of ocular phenotype and negative-type ERG under dark-adapted conditions, a finding that to our knowledge has not been reported before.

Case Report

A 1-year-old boy had appeared normal at birth except for a right eye that was slightly microphthalmic. When he was 1 month old, a diagnosis of retinal detachment was made for the right eye (Fig. 1). His left eye was myopic with a tigroid appearance over the entire retina with pallor of the optic disc. The retinal vessels were tortuous, and the temporal peripheral retina was avascularized in both eyes. A scleral encircling buckle and subsequent vitrectomies were used to repair the retinal detachment in the right eye, but the retina remained detached. Before the surgery, the level of creatinine kinase was elevated (3634 IU/l), and the pediatrician suspected congenital muscular dystrophy despite the lack of any distinctive signs or a family history of muscular dystrophy.

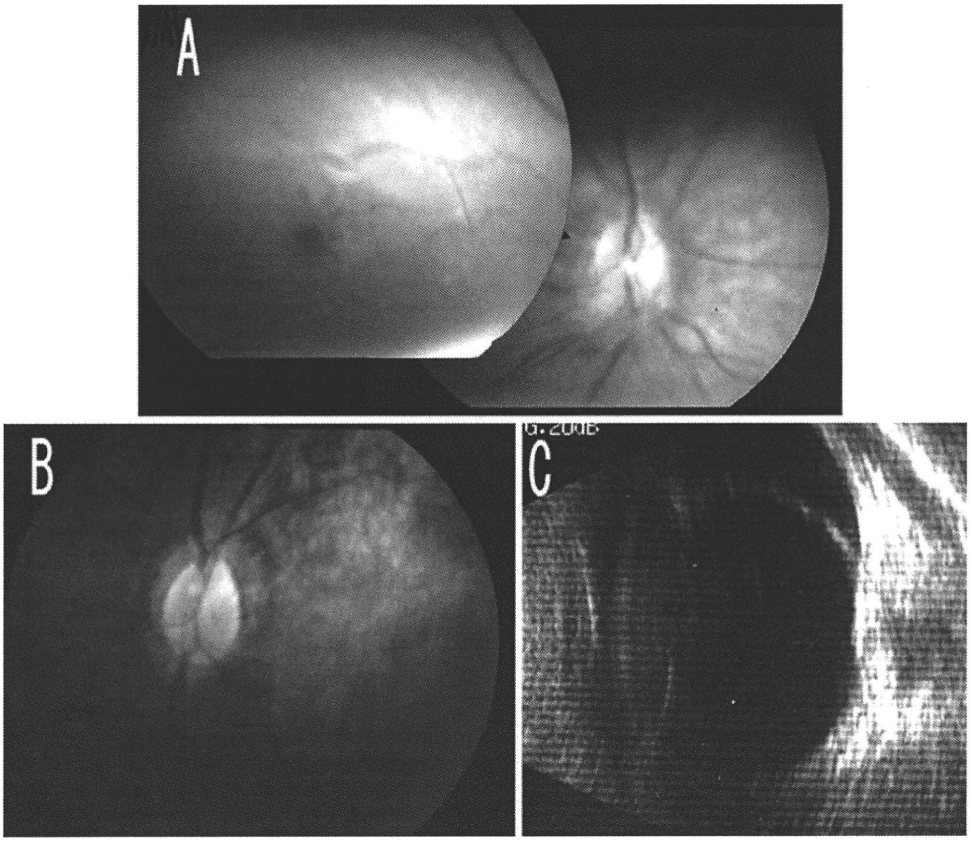

Figure 1A–C. Fundus photographs of our patient with Fukuyama congenital muscular dystrophy (FCMD). **A** Fundus photograph of the right eye showing a temporal retinal detachment involving the macula. **B** Fundus photograph of the left eye showing myopic tigroid appearance with pallor of the optic disc. **C** Ultrasonography showing the retinal detachment in the right eye.

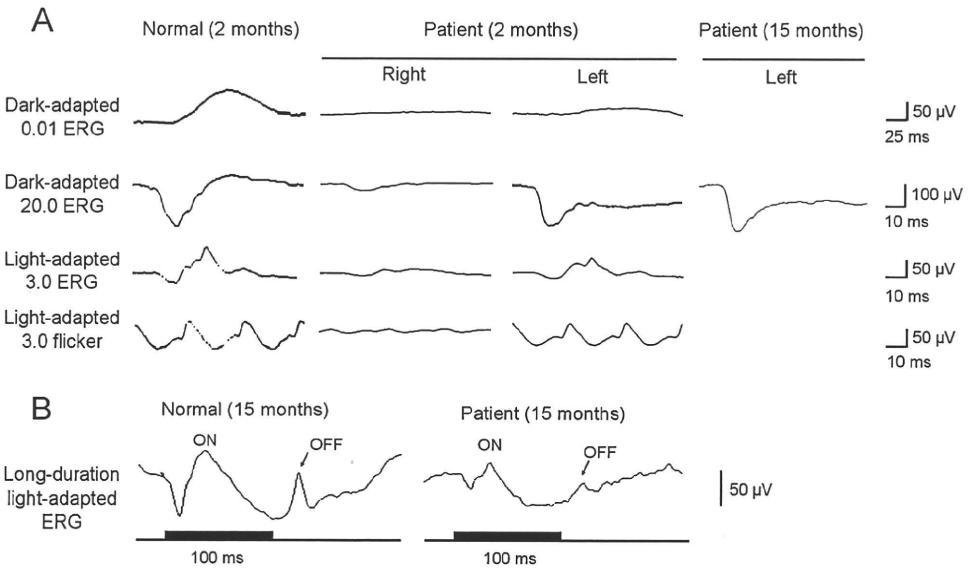

Figure 2A, B. Results of full-field electroretinograms (*ERGs*) using the International Society for Clinical Electrophysiology of Vision-recommended protocol recorded from our patient with FCMD. **A** ERGs recorded in a normal subject at age 2 months (left column), in our patient at 2 months (middle column), and in our patient at age 15 months. The amplitudes of the single-flash cone ERG and 30-Hz flicker ERGs were reduced but better preserved than the rod responses. Note that the maximum rod–cone response (dark-adapted, 20.0 ERG) of our patient showed a "negative" ERG waveform. **B** Light-adapted ERGs elicited by long-duration stimuli in a normal subject at age 15 months (*left*) and in our patient at age 15 months (*right*). Both the ON- and OFF-responses are equally reduced in our patient.

At 5 months, the patient was noted to have muscular weakness and was diagnosed with FCMD. The parents requested genetic testing to confirm the diagnosis. The patient was found to have compound heterozygous mutations in the *FKTN* gene; an insertion mutation in the 3′ noncoding region, and a point mutation, 250C- > T (R47X), in exon 3. The parents were found to be asymptomatic carriers.

During the first vitrectomy under general anesthesia, full-field ERGs were recorded using International Society for Clinical Electrophysiology of Vision-recommended standards (Fig. 2). Because of the retinal detachment, all ERG components in his right eye were severely attenuated. In his left eye, the rod response was decreased to about one-fifth of normal. The a-wave amplitude of the mixed rod–cone ERG was within normal limits, but the b-wave amplitude was smaller than the a-wave amplitude, indicating a negative-type ERG.

Comments

A negative ERG recorded under dark-adapted conditions has not been reported in patients with FCMD and therefore may be a new indication of FCMD. A compound heterozygous mutation in the *FKTN* gene, which occurs infrequently, is most likely the cause of the clinically severe phenotype. This negative-type ERG may be attributable to this less frequent genotype. A similar selective reduction of the b wave was described in patients with muscular dystrophies associated with changes in dystroglycan and dystrophin. The origin of the selective reduction is believed to be a disturbed neurotransmission from the photoreceptors to the ON-bipolar cells.[2]

To determine whether this negative-type ERG was caused by selective impairment of the postsynaptic ON-pathway, we also recorded light-adapted ERGs elicited by long-duration stimuli when our patient was 15 months old. We found that both the ON- and OFF-responses were equally reduced (Fig. 2B). This result is not in accord with the idea that the ON-bipolar cells are selectively disturbed, but an alternative possibility remains that the Müller cells or other neural elements are responsible for the reduction of the b wave because they are also believed to be involved in the generation of the b wave of ERGs.[5]

Acknowledgments. The authors thank Professor Akihiko Tawara for his critical comments and the patient and his parents for their cooperation. This work was partially supported by a Health and Labour Sciences Research Grant (20B-1) for Nervous and Mental Disorders and by Health and Labour Sciences Research Grants for Research on Intractable Diseases from the Ministry of Health, Labour and Welfare of Japan, and by Grants-in-Aid 19592047 and 22591956 for Scientific Research (C) from the Japan Society for the Promotion of Science.

Keywords: *FKTN*, Fukuyama congenital muscular dystrophy, microphthalmia, negative ERG, retinal detachment

Jpn J Ophthalmol
Vol 54: 622–637, 2010

Hiroyuki Kondo[1,2], Kayoko Saito[3], Mari Urano[3], Yukiko Sagara[3], Eiichi Uchio[2], and Mineo Kondo[4]
[1] Department of Ophthalmology, University of Occupational and Environmental Health, Japan, Kitakyushu, Japan; [2] Department of Ophthalmology, Fukuoka University School of Medicine, Fukuoka, Japan; [3] Institute of Medical Genetics, Tokyo Women's Medical University, Tokyo, Japan; [4] Department of Ophthalmology, Nagoya University Graduate School of Medicine, Nagoya, Japan

Received: February 24, 2010 / Accepted: June 29, 2010
Correspondence to: Hiroyuki Kondo, Department of Ophthalmology, University of Occupational and Environmental Health, Japan, 1-1 Iseigaoka, Yahatanishi-ku, Kitakyushu 807-8555, Japan
e-mail: kondohi@med.uoeh-u.ac.jp

DOI 10.1007/s10384-010-0875-0

References

1. Fukuyama Y, Osawa M, Suzuki H. Congenital progressive muscular dystrophy of the Fukuyama type—clinical, genetic and pathological considerations. Brain Dev 1981;3:1–29.
2. Santavuori P, Somer H, Sainio K, et al. Muscle-eye-brain disease (MEB). Brain Dev 1989;11:147–153.
3. Chijiiwa T, Nishimura M, Inomata H, Yamana T, Narazaki O, Kurokawa T. Ocular manifestations of congenital muscular dystrophy (Fukuyama type). Ann Ophthalmol 1983;15:921–923, 926–928.
4. Mishima H, Hirata H, Ono H, Choshi K, Nishi Y, Fukuda K. A Fukuyama type of congenital muscular dystrophy associated with atypical gyrate atrophy of the choroid and retina. A case report. Acta Ophthalmol (Copenh) 1985;63:155–159.
5. Ueda H, Gohdo T, Ohno S. Beta-dystroglycan localization in the photoreceptor and Muller cells in the rat retina revealed by immunoelectron microscopy. J Histochem Cytochem 1998;46:185–191.

Case of a Japanese Patient with X-linked Ocular Albinism Associated with the *GPR143* Gene Mutation

Albinism is an inherited disorder characterized by a reduction or absence of melanin in the hair, skin, and eyes. Albinism can be divided into two broad categories: oculocutaneous albinism and ocular albinism.[1] X-linked ocular albinism (XLOA) is characterized by nystagmus, decreased visual acuity, strabismus, fundus hypopigmentation, macular hypoplasia, and iris hypopigmentation with translucency. It is caused by mutations in the G protein-coupled receptor 143 (*GPR143*) gene (OMIM 300808), originally referred to as the *OA1* gene, which is located at Xp22.32.[2] The fundus of female carriers has a mosaic pattern of pigmentation and depigmentation, which helps in diagnosing XLOA.

We report on a Japanese boy with XLOA whose hair and skin appeared to be hypopigmented, causing some of the referring doctors and his parents to be concerned that he was suffering from oculocutaneous albinism. We detected a *GPR143/OA1* gene mutation, making this the first report of this mutation in Japan.

Case Report

The patient was a 4-month-old boy who had been born by normal delivery with a birth weight of 3148 g. His parents noticed that both his irides were blue and his eye movements appeared abnormal from birth. They consulted a pediatrician, who suspected oculocutaneous albinism. The patient was referred to us when he was 4 months old.

No family history of albinism was reported. His hair was mostly light brown, and his skin color was fair for a Japanese individual. He showed pendular horizontal nystagmus but could follow a slowly moving target. His refraction was –0.50 D = cyl –2.00 D Ax 180° (OD) and –0.50 D = cyl –1.50 D Ax 180° (OS). Slit-lamp examination showed that both irides were light brown (Fig. 1A, B). Bilateral foveal hypoplasia was present, and the ocular fundus was albinotic (Fig. 1C, D). Because his mother's fundus showed a mosaic pattern in the midperiphery, XLOA was diagnosed (Fig. 1E, F). He was also seen by a pediatrician of the Hamamatsu University School of Medicine, who diagnosed oculocutaneous albinism rather than ocular albinism (Fig. 1G, H). Because of the discrepancy in diagnoses, his parents wanted the diagnosis confirmed so as to know whether his skin needed to be protected from ultraviolet exposure.

After genetic counseling, the parents agreed to a genetic examination of their child and of themselves. The molecular genetics study was approved by the Institutional Review Board for Human Genetics and Genomic Research of Hamamatsu University School of Medicine. Nine exons and the surrounding regions of the *GPR143* gene were amplified by polymerase chain reaction (PCR) and directly sequenced. A splice mutation at the junction between exon 5 and intron 5, c.658+1G>A, was detected in the patient (Fig. 2). A heterozygous mutation was detected in his mother, but not in his father. The polymorphisms c.251–135C>T and c.767+10C>G were also detected in the patient.

Comments

This is the first report of a Japanese XLOA patient with a *GPR143* mutation. Various types of mutations in *GPR143* have been identified in Caucasian and Chinese populations. The splice mutation c.658+1G>A that we described here has been previously reported.[3]

Most Japanese patients with XLOA have brown irides that show no translucency, nonalbinotic fundi with moderate pigmentation, and normal skin and hair color.[4] However, the iris in our patient was light brown and the fundus was albinotic. His hair color was mostly light brown, and his skin color was fair for a Japanese individual. The skin and hair pigmentation in Caucasians with ocular albinism can be in the normal range but is frequently lighter in color than that of their siblings without XLOA. Recently, a Chinese family with XLOA and a *GPR143* mutation was reported to have iris hyperpigmentation.[5] Although the amount of pigment